Indonesian Physical Review
Volume 08 Issue 01, January 2025
P-ISSN: 2615-1278, E-ISSN: 2614-7904

The Effect of Calcination Temperature and Holding Time on Structural Properties of Calcia Powders Derived from Eggshell Waste

Budi Prayitno[1*], Musyarofah[2*], Gusti Umindya Nur Tajalla[3], Azmia Rizka Nafisah[4], Siti Norhidayah[1], Siska Ayu Kartika[1]

[1] *Department of Mechanical Engineering, Universitas Balikpapan, Indonesia*
[2] *Department of Physics, Institut Teknologi Kalimantan, Indonesia*
[3] *Department of Material and Metallurgy Engineering, Institut Teknologi Kalimantan, Indonesia*
[4] *Department of Chemistry Engineering, Institut Teknologi Kalimantan, Indonesia*

Corresponding Authors E-mail: budi.prayitno@uniba-bpn.ac.id, musyarofah@lecturer.itk.ac.id

Article Info

Article info:
Received: 18-12-2024
Revised: 11-01-2025
Accepted: 21-01-2025

Keywords:
Calcia; Calcination; Holding time; Microstructure; Structure; Temperature

How To Cite:
B. Prayitno, Musyarofah, G. U. N. Tajalla, A. R. Nafisah, S. Norhidayah, and S. A. Kartika, "The Effect of Calcination Temperature and Holding Time on Structural Properties of Calcia Powders Derived from Eggshell Waste", Indonesian Physical Review, vol. 8, no. 1, p 281-299, 2025.

DOI:
https://doi.org/10.29303/ipr.v8i1.450.

Abstract

This study investigates the effects of calcination temperature and holding time on the structural properties of calcia (CaO) powders. The raw material used in this study is chicken eggshell waste, which was cleaned, dried, ground, and sieved for uniform particle size. The synthesis of calcia powder was performed by calcining the powder at 900 ℃ and 1000 ℃ for 5, 10, and 15 hours. XRD, BET, and SEM analyses were employed to evaluate crystal structure, textural properties, and microstructure of the calcined powders. The Rietveld analysis reveals the identified crystalline phases were calcia up to 95.6 mol% and calcium hydroxide as secondary phase. Results indicate that higher calcination temperatures and extended holding times increase particle size and reduce BET surface area, significantly altering pore size distribution. Specifically, elevated temperatures promote sintering and grain growth, leading to smaller average pore radii and decreased total pore volume. The BET surface area ranges from 7.431 m^2/g to 1.772 m^2/g for samples calcined at 900 ℃ and from 3.202 m^2/g to 0.711 m^2/g for samples calcined at 1000 ℃. Correspondingly, the average particle radius increases from 183.51 nm to 769.55 nm at 900 ℃ and from 425.83 nm to 1918.10 nm at 1000 ℃ as the holding time extends. BJH analysis reveals that longer holding times broaden pore size distribution due to the merging of smaller pores.

Introduction

The structural characteristics of calcium oxide (CaO) powders, commonly referred to as calcia, derived from calcium-rich precursors such as eggshell biowaste, have garnered considerable interest due to their broad range of applications in fields such as catalysis [1], anti-microbial ceramics [2], environmental remediation [3], [4], etc. The ability to control these structural characteristics through precise manipulation of synthesis parameters is crucial for enhancing the performance and functionality of calcia-based materials.

Calcination, a thermal treatment process involving the heating of materials in the presence of air, plays a pivotal role in determining the final properties of calcia powders. Key parameters of the calcination process, specifically temperature and holding time, significantly impact structural properties such as the phase composition, lattice parameters, crystallinity, textural properties (including average pore radius, total pore volume, surface area, average particle radius, and pore radius distribution), and microstructure of the resulting ceramic materials [5], [6]. Understanding the effects of these parameters is essential for optimizing the synthesis process to produce calcia powders from eggshell biowaste, a readily available and sustainable raw material.

Previous studies [7] on the synthesis of calcium oxide (CaO) have highlighted significant challenges that impact the quality and applicability of the final product. One of the primary issues is the sensitivity of the synthesis process to variations in calcination temperature and holding time, which play a crucial role in determining key structural properties such as particle size, pore distribution, and crystallinity. These variations can lead to inconsistencies in product performance, particularly in applications requiring precise control over material properties. Other previous studies have demonstrated the potential of eggshells as a sustainable source of calcia. For example, recent research by Prayitno et al [8] and Alobaidi et al [9] have shown that calcination of eggshells at high temperatures results in the formation of calcia. However, these studies primarily focused on single temperature and holding time conditions, leaving a gap in the understanding of the combined effects of varying calcination temperatures and holding times on the structural characteristics of calcia powders. In addition to eggshell biowaste, other calcium-rich biowaste materials have been investigated for the synthesis of calcia. For instance, eggshells, seashells and bones have been explored as alternative sources. The studies by Ling et al [10] highlight that these biowastes can be effectively converted into calcia through several synthesis methods, with each type of biowaste exhibiting unique structural properties depending on the process conditions.

In this study, we address these limitations by systematically optimizing the calcination parameters, focusing on temperature and holding time, to achieve a more efficient transformation of eggshell waste into CaO powders. By refining these conditions, our research aims to produce CaO with enhanced structural properties, such as higher purity levels, consistent particle size, and improved porosity, which are essential for its application in various fields, including catalysis, environmental remediation, and biomedical uses. This approach not only improves the quality of the final product but also contributes to sustainable waste management by valorizing eggshell waste as a valuable raw material. Despite the extensive body of research on the synthesis and characterization of calcia powders from various biowaste materials, a comprehensive study focusing on the effects of specific calcination temperatures and holding times on their structural characteristics remains limited. This study aims to fill this gap by systematically investigating the impact of two

calcination temperatures (900 °C and 1000 °C) and three holding times (5, 10, and 15 hours) on the structural attributes of calcia powders synthesized from eggshell biowaste. Using advanced characterization techniques such as X-ray diffraction (XRD) for phase composition and lattice parameters, scanning electron microscopy (SEM) for microstructural analysis, and Brunauer-Emmett-Teller (BET) surface area analysis for textural properties, this research provides a detailed understanding of how calcination parameters influence the structural characteristics of calcia powders. The findings from this study will contribute to the optimization of calcination processes, thereby enhancing the application potential of calcia powders derived from sustainable biowaste sources.

Experimental Method

This study utilized chicken eggshells collected from household waste as the primary material. Chicken eggshells were chosen due to their abundant availability and ease of acquisition as a byproduct of daily household consumption. Using household waste as a raw material aligns with efforts to reduce waste and utilize available resources more efficiently. The eggshells were cleaned thoroughly with deionized water to remove any organic residues and then dried at 100 °C for 24 hours. The dried eggshells were then ground into fine powder using a mechanical grinder and sieved to obtain a uniform particle size distribution. The synthesis of calcia powder was carried out through a calcination process. The ground eggshell powder was subjected to calcination in a muffle furnace with two different calcination temperatures: 900 °C and 1000 °C. For each temperature, three different holding times were tested: 5 hours, 10 hours, and 15 hours. The calcination process involved heating the samples at a controlled rate of 10 °C per minute until the desired temperature was reached, followed by maintaining the temperature for the specified holding time. After the holding period, the furnace was allowed to cool naturally to room temperature.

The phase composition and crystal lattice parameters of the calcined powders were determined using X-ray diffraction (XRD) analysis. The XRD patterns were obtained using a Bruker D8 Advanced X-ray diffractometer with Cu-Kα radiation (λ = 1.5406 Å) over a 2θ range of 5 to 120° at a scanning rate of 0.02° per second. The Rietveld method was employed using *Match!* and *Rietica* software to refine the XRD data and extract detailed information on phase composition and lattice parameters [11], [12]. The textural properties of the calcined powders were determined using a BET Surface Area & Pore Size Analyzer (NOVATouch LX4). The samples were degassed at 300 °C for 3 hours prior to analysis to remove any adsorbed moisture and gases. Nitrogen adsorption-desorption isotherms were obtained at liquid nitrogen temperature (77 K), and the surface area was calculated using the Brunauer-Emmett-Teller (BET) method. The pore size distribution was derived from the adsorption branch of the isotherm using the Barrett-Joyner-Halenda (BJH) method. The microstructural characteristics of the calcined powders were examined using scanning electron microscopy (SEM). The samples were mounted on aluminum stubs and coated with a thin layer of gold to enhance conductivity. SEM images were captured using a Phenom X5 Pro scanning electron microscope operating at an accelerating voltage of 15 kV. The microstructural analysis provided insights into the morphology of the calcined powders.

Result and Discussion

Crystal Structure Analysis

The XRD patterns presented in Figures 1 and 2 depict the diffraction profiles of calcined chicken eggshell powders subjected to varying holding times of 5, 10, and 15 hours at temperatures of 900 °C and 1000 °C. The qualitative phase analysis conducted on these patterns has identified the primary phase as calcia (calcium oxide, CaO, COD No. 1-011-095), which crystallizes in the space group *Fm-3m*. This indicates that calcium oxide is the dominant crystalline phase present after the calcination process under the specified conditions. In addition to the primary calcia phase, a secondary phase was detected, characterized by smaller peaks in the XRD patterns. This secondary phase has been identified as calcium hydroxide ($Ca(OH)_2$, COD No. 9-000-113, space group *P-3m1*). The presence of calcium hydroxide suggests that some of the calcium oxide may have reacted with atmospheric moisture during sample preparation or handling, forming the hydroxide phase.

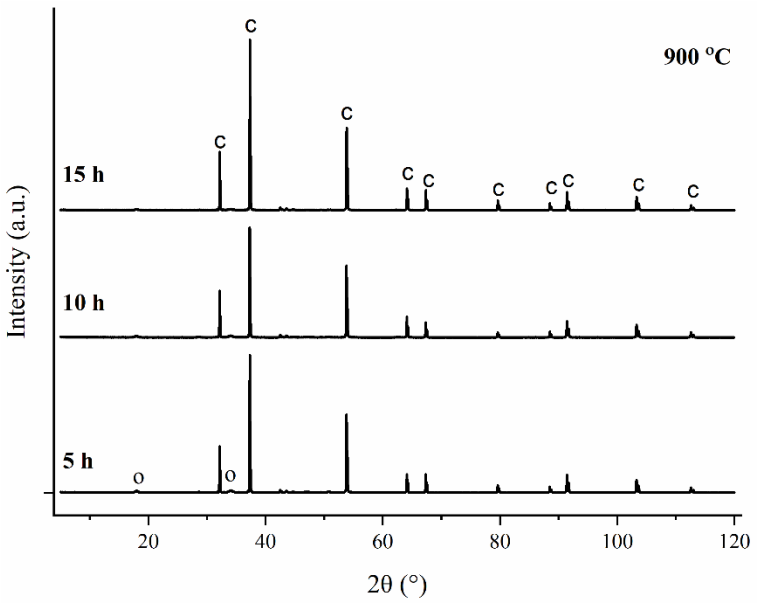

Figure 1. X-ray diffraction patten (Cu-Kα) of calcia powders calcined at 900 °C with variation of holding time for 5, 10, and 15 hours

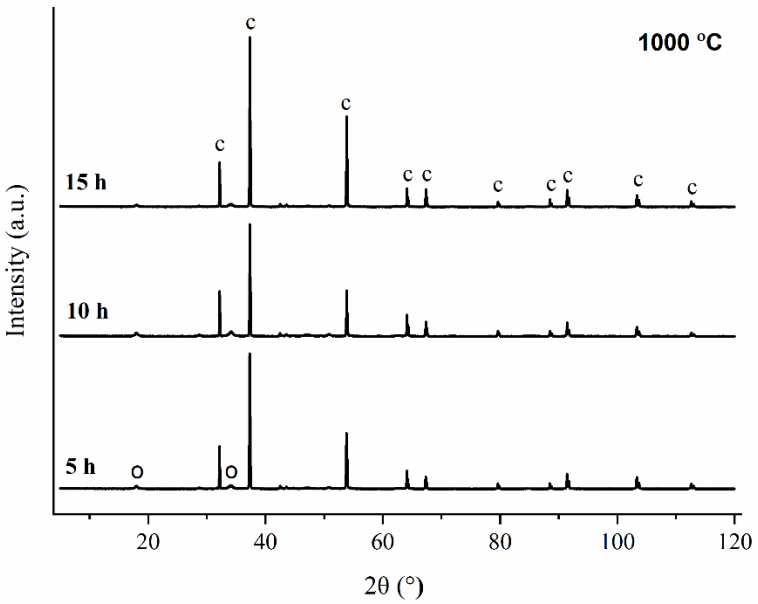

Figure 2. X-ray diffraction patten (Cu-Kα) of calcia powders calcined at 1000 °C with variation of holding time for 5, 10, and 15 hours

Both phases, calcium oxide and calcium hydroxide, were consistently observed across all samples regardless of the calcination temperature (900 °C and 1000 °C) and the holding time variations (5, 10, and 15 hours). This consistent presence indicates that the formation of these phases is robust under the given experimental conditions. The dominant peaks corresponding to calcium oxide imply that the primary thermal decomposition product of the eggshells is calcium oxide, while the secondary peaks for calcium hydroxide suggest a minor hydration reaction. A detailed explanation to elucidate the phase formation mechanism in calcined eggshell powder and the influence of calcination parameters will be provided subsequently.

The formation of calcia from calcium carbonate ($CaCO_3$) in eggshells through calcination at a temperature of 900 and 1000 °C involves a thermal decomposition reaction. Initially, as the temperature increases, the eggshells lose moisture and any organic materials present at approximately 692 °C [13]. Calcium carbonate was converted into calcia at 690 and 850 °C, the thermal energy provided is sufficient to break the chemical bonds in calcium carbonate, resulting in the formation of calcia and the release of carbon dioxide (CO_2) gas then completely regenerated at 1000 °C [14]. This decomposition reaction can be represented by the Eq. (1).

$$CaCO_3 \rightarrow CaO + CO_2 \qquad (1)$$

During calcination, significant structural changes occur within the eggshells. The release of carbon dioxide gas creates voids in the material, leading to the development of a porous structure in the resulting calcia. This increased porosity enhances the reactivity of the calcia, making it more suitable for various industrial applications [15]. The kinetics of this decomposition reaction are influenced by factors such as temperature, particle size, and the presence of impurities [16], [17]. At high temperature, the reaction rate is high enough to ensure the complete decomposition of calcium carbonate. Smaller particle sizes decompose more rapidly due to their larger surface area, which facilitates the reaction. The final product

of this calcination process is calcium oxide, a white and highly reactive powder. The purity and reactivity of the calcia depend on the thoroughness of the calcination process and the extent to which impurities are removed. Proper control of the calcination temperature and duration is crucial to obtaining high-purity calcia.

At the calcination temperature of 900 and 1000 °C, along with the formation of calcia, calcium hydroxide can also form. This occurs due to the interaction between the calcia produced and any available moisture or water vapor in the atmosphere or within the material being calcined. The mechanism of calcium hydroxide formation involves a hydration reaction represented by the Eq. (2).

$$CaO + H_2O \rightarrow Ca(OH)_2 \quad (2)$$

During the calcination process, especially at temperatures around 1000 °C, calcia is very reactive and readily reacts with water molecules to form calcium hydroxide. This reaction is exothermic, meaning it releases heat as the calcia reacts with water vapor or moisture. The formation of calcium hydroxide alters the chemical composition of the material and influences its properties. The presence of calcium hydroxide alongside calcia after calcination indicates that hydration has occurred due to the exposure of calcia to moisture. This hydration process can affect the material's stability, reactivity, and applications [18]. In industrial settings, controlling moisture levels during and after calcination is crucial to regulate the formation of calcium hydroxide and optimize the desired properties of the final product, whether it be calcia, calcium hydroxide, or a mixture of both. Thus, at 900 and 1000 °C, while calcia is primarily formed from calcium carbonate during calcination, the presence of water vapor or moisture can lead to concurrent formation of calcium hydroxide through a straightforward hydration reaction with calcia.

Analysis of the X-ray diffraction (XRD) patterns in Figures 3 and 4 shows that the diffraction peaks at 2θ positions around 32.0° and 32.5°, which are related to the crystallinity of calcia, do not experience significant changes in width despite variations in calcination temperature and time. Peak broadening in X-ray diffraction generally reflects the crystallite size; a wider peak indicates smaller crystallites, and vice versa. In this context, the unchanged peak width indicates that the crystallite size of calcia remains constant over the range of calcination temperatures and times tested. This finding is consistent with previous studies showing that calcination temperature and time affect crystallite size. For example, studies on geikielite powder showed that increasing the calcination temperature tended to increase the average crystallite size. The smallest average crystallite size of 18 nm was obtained at 600 °C for 4 hours, while the largest size was 189 nm at 800 °C [19]. However, in our qualitative study, temperature variations up to 1000 °C and holding times up to 15 hours did not result in significant changes in the calcia crystallite size, as indicated by the unchanged XRD peak widths. This crystallite size stability may be due to several factors [20]. First, the chemical composition and intrinsic properties of the original material, such as eggshell, may hinder crystallite growth during calcination. Second, the calcination conditions used may not have reached the threshold required to trigger further crystallite growth. In addition, the presence of impurities or other compounds in the original material may inhibit the ion diffusion required for crystallite growth. A thorough understanding of the effect of calcination

parameters on the calcia crystallite size is essential, especially in applications that require specific material properties. By knowing that within the range of tested parameters the crystallite size remains stable, researchers and practitioners can design a more efficient calcination process that suits the needs of a particular application. For further modification, it may be necessary to consider additional parameters or other treatments that can affect the size and properties of calcia crystallites.

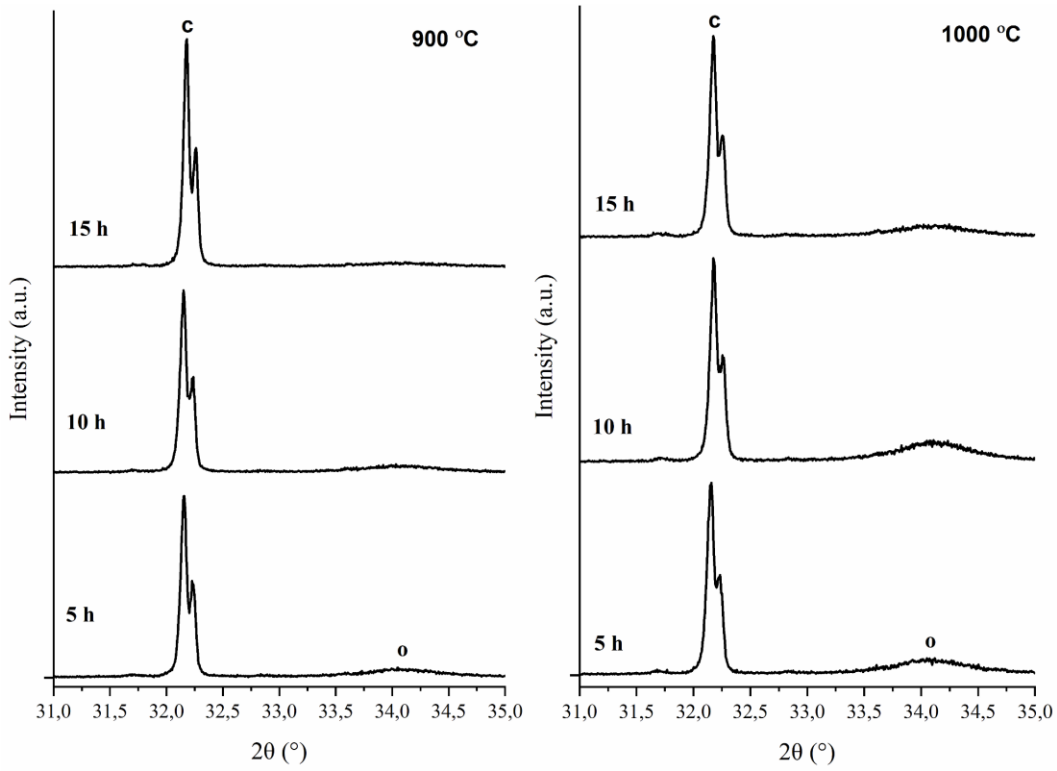

Figure 3. XRD peak broadening details of the calcined calcia powders with variation of calcination holding time

However, the calcination temperature and holding time do influence the ratio of the peak heights of calcia and calcium hydroxide. Specifically, as the holding time increases, there is a noticeable decrease in the peak height of calcium hydroxide. This reduction in peak height indicates a decrease in the phase composition of calcium hydroxide, suggesting that prolonged exposure to high temperatures reduces its presence. This may be due to the dehydration of calcium hydroxide or its further transformation into other phases. Conversely, increasing the calcination temperature results in a higher peak height of calcium hydroxide, indicating an increase in its phase composition. This implies that higher temperatures promote the formation or stabilization of calcium hydroxide, possibly due to enhanced reactivity of calcia with atmospheric moisture during the cooling process or post-calcination handling.

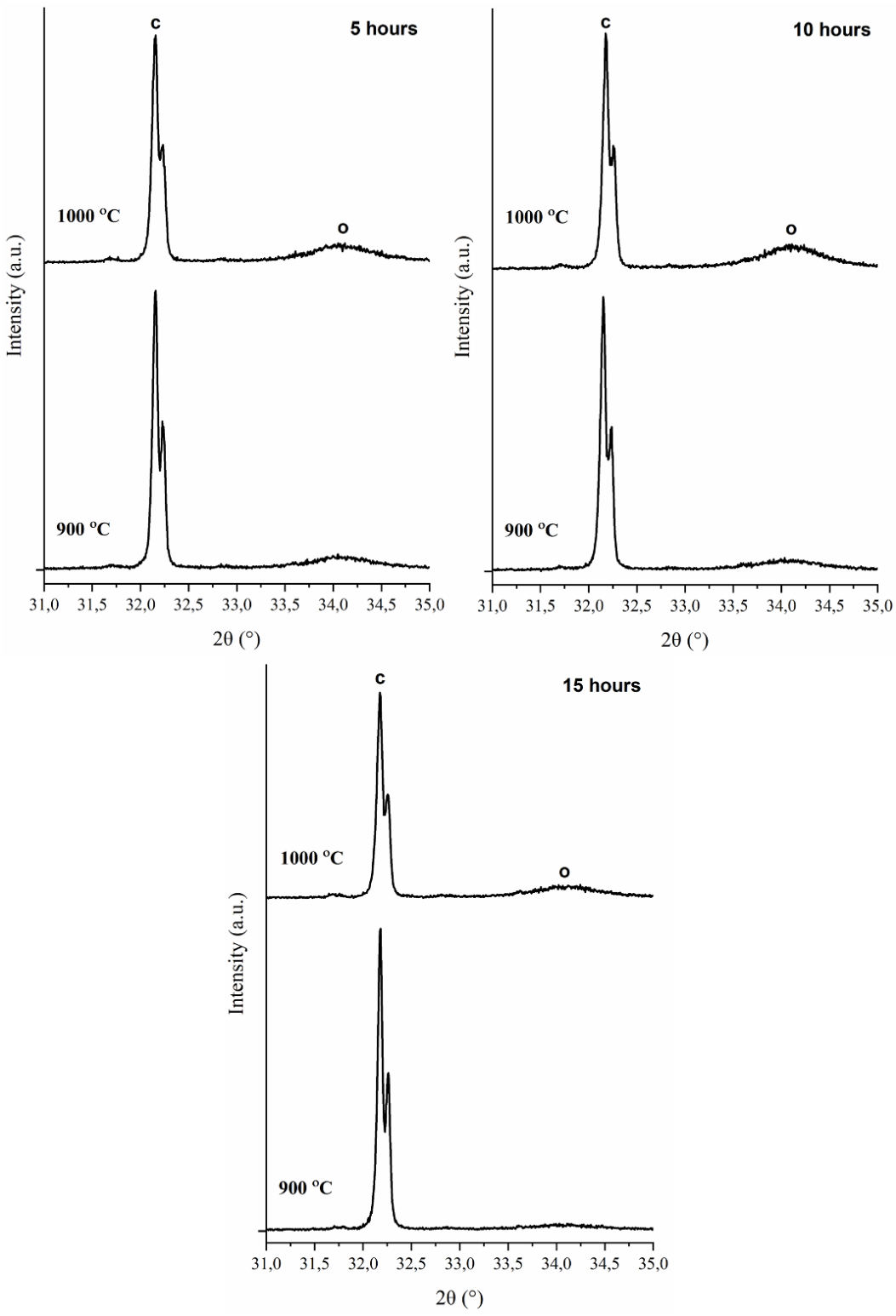

Figure 4. XRD peak broadening details of the calcined calcia powders with variation of calcination temperature

These observations suggest that while the crystallite size of calcia remains stable, the phase composition and relative abundance of calcium hydroxide are significantly influenced by both calcination temperature and holding time. The results imply that the reactivity of calcia to form calcium hydroxide is modulated by these calcination parameters. Higher temperatures may increase the reactivity, leading to more calcium hydroxide formation, while longer holding times may decrease its presence, likely due to prolonged thermal treatment reducing the amount of calcium hydroxide through dehydration or transformation into other phases [21].

Quantitative phase analyses of the XRD data, conducted using the Rietveld-based Rietica software, determined the relative mole fractions of the phases for all samples, as detailed in Table 1. At a calcination temperature of 900 and 1000°C and varying holding times (5, 10, and 15 hours), the calcium carbonate is completely decomposed, leading to the formation of calcia. The composition of calcia formed is up to 95.59% and 93.75% and by mole, respectively. These results demonstrate that a longer holding time results in higher purity of calcia, irrespective of the calcination temperature. This occurs because the extended holding time allows for a more complete transformation of calcium carbonate into calcia, reducing the presence of secondary phases like calcium hydroxide. As holding time increases, the interactions between calcia and moisture are minimized, thereby suppressing the hydration process and resulting in minimal formation of calcium hydroxide. In practice, controlling both the calcination temperature and holding time is crucial for optimizing the purity of calcia and managing the hydration process. Higher calcination temperatures and longer holding times both contribute to the increased purity of calcia by enhancing the decomposition of calcium carbonate and reducing the likelihood of hydration. This dual approach ensures that the final product has a higher calcia content with minimal calcium hydroxide impurities, thereby improving the material's overall quality and suitability for various applications.

Table 1. Rietveld-derived phase composition and lattice parameters (volume cell) of the calcined powders (referred to Figures 1 and 2) using *Rietica* software. Numbers in parentheses represent estimated standard deviation to associated average value at its least significant level.

Sample	Phase Composition (mol%)		Lattice Parameters of Calcia
	Calcia	Calcium hydroxide	***a=b=c* (Å)**
C900-5h	90.39 (2)	9.61 (1)	4.8102 (1)
C900-10h	92.11 (2)	7.89 (1)	4.8103 (2)
C900-15h	95.59 (3)	4.41 (2)	4.8106 (2)
C1000-5h	87.56 (4)	12.44 (1)	4.8104 (2)
C1000-10h	89.53 (2)	10.47 (1)	4.8104 (2)
C1000-15h	93.75 (4)	6.25 (1)	4.8106 (2)

The stability of crystal lattice parameters in calcia during variations in calcination holding time is typically observed due to the nature of the crystal structure itself. Calcia crystallizes in a cubic crystal system with a rock salt structure (often referred to as face-centered cubic, FCC). This crystal structure is inherently stable, with well-defined lattice parameters that remain consistent under different calcination conditions, including temperature and holding time

variations. Changes in calcination conditions primarily affect the crystallite size and degree of crystallinity rather than the fundamental lattice parameters [22].

Textural Structure Analysis

Adsorption-desorption isotherm curves for the studied calcined calcia powders are presented in Figure 5. When the amount of N_2 adsorbed was plotted against the relative pressure, all calcia-based samples exhibited IUPAC-classified BET type-IVa isotherms, indicating the presence of mesoporous materials with pore sizes ranging from 2 to 50 nanometers [14]. These isotherms provide valuable information about the pore structure and adsorption behavior of the material. Type-IVa isotherms exhibit a sigmoidal shape with three distinct regions [23]. At low relative pressures ($P/P_0 < 0.1$), monolayer adsorption of nitrogen molecules occurs on the surface of the material. At intermediate relative pressures ($0.1 < P/P_0 < 0.3$), multilayer adsorption takes place, where multiple layers of nitrogen molecules accumulate. At higher relative pressures ($P/P_0 > 0.3$), capillary condensation begins within the mesopores, leading to a steep increase in the amount of adsorbed nitrogen. The desorption branch of the isotherm does not follow the same path as the adsorption branch, resulting in a hysteresis loop. This discrepancy is due to the delayed evaporation of nitrogen from the mesopores during desorption, influenced by the pore structure and connectivity. The presence of a hysteresis loop at higher relative pressures during desorption is a key feature of type-IVa isotherms, indicative of capillary condensation within the mesopores and often classified according to its shape.

Additionally, the N_2 adsorption-desorption isotherm measurements showed IUPAC-classified H3 type hysteresis loops [24]. These loops are typically associated with materials exhibiting non-rigid aggregates of plate-like particles or slit-shaped pores. The H3 hysteresis loop does not exhibit a limiting adsorption at high relative pressures, indicating the presence of mesopores. It is typically found in the middle to high relative pressure range (P/P_0). This loop is linked to slit-like or plate-like pores where capillary condensation occurs, with the desorption process not following the same path as adsorption due to the complex pore structure and connectivity. The hysteresis results from the different mechanisms of adsorption and desorption in mesopores, where adsorption involves the filling of mesopores by capillary condensation, and desorption may involve evaporation from smaller pores first, followed by larger pores.

The surface area of the calcined samples is determined using the Brunauer-Emmett-Teller (BET) theory by the adsorption technique. Nitrogen molecules act as adsorbates, forming a layer around the pores and surfaces of the samples to assess their surface area and porosity [25]. Detailed surface characteristics were analyzed using BET characterization to estimate the specific surface area of calcia powders, as summarized in Table 2. The calcination holding time has a significant impact on the structural properties of calcined materials, including average pore radius, total pore volume, BET surface area, and average particle radius. Prolonged calcination generally leads to an increase in the average pore radius. This is because extended heating allows for the growth and merging of smaller pores into larger ones [26]. Conversely, shorter calcination times tend to preserve smaller pore sizes since there is less time for significant pore growth. Furthermore, the total pore volume can either increase or decrease

with varying calcination holding times. Initially, as volatile components are removed during calcination, the total pore volume might increase. However, with extended holding times, the total pore volume often decreases, where pores collapse or merge, thus reducing the overall pore volume.

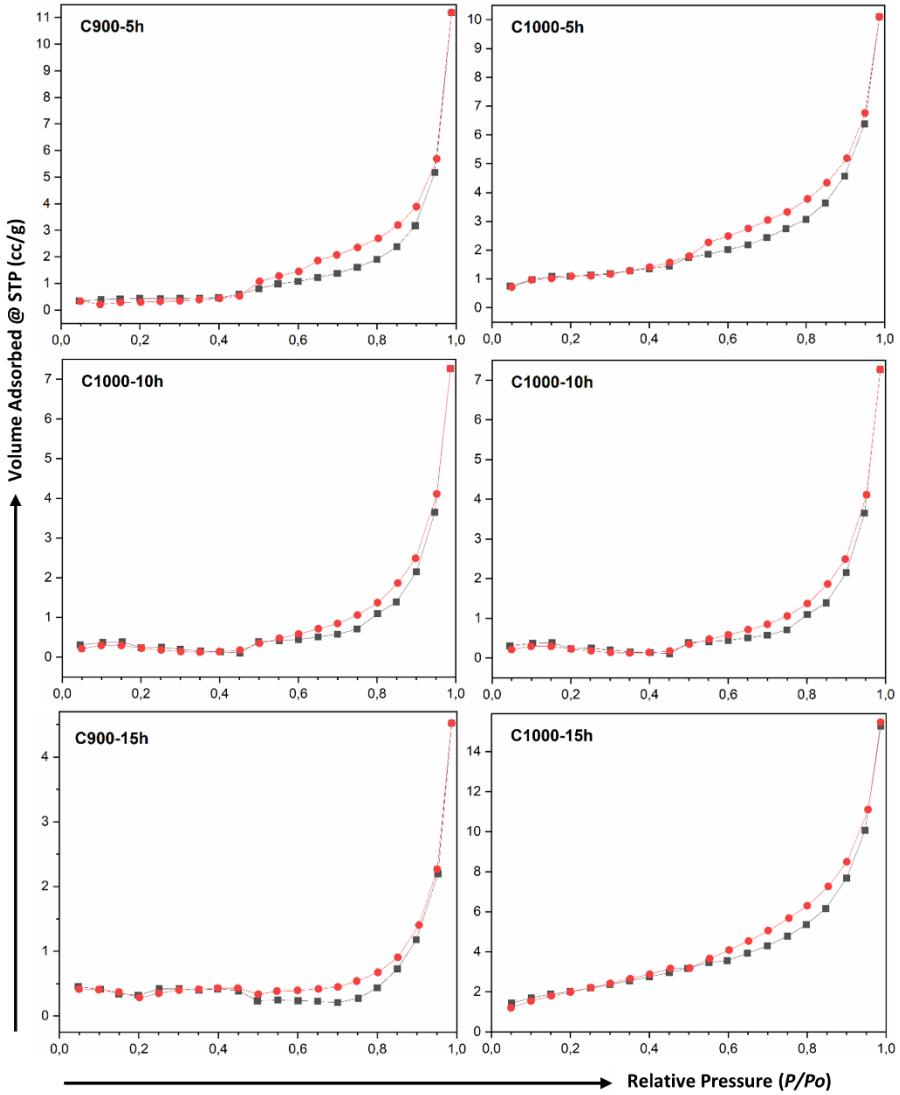

Figure 5. N_2 adsorption-desorption isotherms of the calcined calcia powders with variation of calcination temperature and holding time (red line: desorption, black line: adsorption)

The BET surface area usually decreases with longer calcination holding times [27], [28]. This reduction occurs because prolonged heating promotes grain growth and pore collapse, which reduces the surface area. In contrast, shorter calcination times help maintain a higher BET surface area since the pore structure remains relatively intact, retaining the high surface area characteristic of mesoporous materials. Similarly, the average particle radius increases with longer calcination holding times due to grain growth. Prolonged heating allows particles to coalesce and grow larger [26]. On the other hand, shorter calcination times result in smaller average particle

radii as the particles do not have sufficient time to grow significantly, thus retaining their finer sizes. In summary, optimizing the calcination holding time is crucial to achieve desired structural properties in calcined materials. Longer calcination times tend to increase the average pore and particle sizes while decreasing the BET surface area and potentially reducing total pore volume due to sintering effects. Shorter calcination times generally preserve smaller pore and particle sizes, higher surface areas, and higher total pore volumes by minimizing sintering and growth processes.

Table 2 Average pore size, total pore volume, surface area, and average particle size summary using BET-Multi-point method

Sample	Average pore radius (nm)	Total pore volume $\times 10^{-2}$ (cc/g)	BET surface area (m^2/g)	Average particle radius (nm)
C900-5h	6.456	1.335	7.431	183.51
C900-10h	7.293	1.748	4.293	317.61
C900-15h	12.719	0.562	1.772	769.55
C1000-5h	1.108	2.399	3.132	435.44
C1000-10h	8.416	1.566	3.202	425.83
C1000-15h	15.795	1.127	0.711	1918.10

Calcination temperature has a notable impact on the average pore radius of the calcined samples at 900 and 1000 °C. As the temperature increases, enhanced sintering and grain growth tend to reduce the average pore radius. The thermal energy at higher temperatures facilitates the diffusion of atoms, leading to the closure of smaller pores and coarsening of the pore structure [26]. This reduction in average pore radius is particularly evident in porous materials where maintaining an optimal pore size is crucial for applications such as catalysis and adsorption. However, the specific effect on pore radius can vary depending on the material and the initial pore structure.

The total pore volume generally decreases with increasing calcination temperature. Higher temperatures promote the densification of the material through sintering, which reduces the overall porosity [11]. This densification process decreases the number of open pores, thereby reducing the total pore volume. Additionally, the decomposition of volatile components and burnout of organic templates at higher temperatures can further reduce pore volume. Maintaining an appropriate total pore volume is essential for applications that rely on high porosity, such as filtration and gas storage.

The BET surface area, which measures the specific surface area of a material, is also influenced by calcination temperature. Generally, as calcination temperature increases, the BET surface area decreases. This reduction occurs because higher temperatures cause sintering and grain growth, leading to a decrease in the surface area exposed by smaller pores [26]. The closure of mesopores at elevated temperatures contributes to this decline in surface area. Calcination temperature has a direct impact on the average particle radius as well. As the temperature increases, particles tend to grow larger due to the increased mobility of atoms and the coalescence of smaller particles [11]. This growth is a result of heating, where smaller particles merge to form larger ones, leading to an increase in the average particle radius. The rate of

particle growth depends on the material and the specific calcination conditions [29]. Control over particle size is crucial for applications that require specific particle size distributions, such as in pharmaceuticals and nanotechnology.

BJH (Barrett, Joyner, and Halenda) analysis is used to assess the distribution of pore sizes in calcined calcia powders, see Figure 6. These powders generally exhibit irregular pore-size distributions, typically showing a unimodal distribution in the small mesopore range (<10 nm). The calcination holding time significantly influences the pore size distribution. Longer holding times tend to broaden the pore size distribution due to the growth and merging of smaller pores into larger ones [29]. This can lead to a more heterogeneous distribution as smaller pores coalesce into larger mesopores. Conversely, shorter holding times help maintain a narrower pore size distribution by preserving the original smaller pore sizes and minimizing the coalescence and growth processes. Thus, optimizing the calcination holding time is crucial to achieving the desired pore size distribution, with longer times potentially resulting in a wider range of pore sizes and shorter times maintaining a more uniform, unimodal distribution in the smaller mesopore range.

In addition to holding time, calcination temperature also plays a crucial role in determining the distribution of pore sizes. Higher calcination temperatures generally lead to a significant alteration in the pore size distribution due to enhanced sintering and grain growth. As the temperature increases, the thermal energy promotes the diffusion of atoms, causing the smaller pores to merge and form larger pores [30]. This results in a shift of the pore size distribution towards larger mesopores and macropores, making the distribution broader and more heterogeneous. The increased temperature can also cause the collapse of some smaller pores, further contributing to a more varied pore size distribution. Conversely, at lower calcination temperatures, the sintering process is less pronounced, which helps preserve the smaller pores and maintains a narrower pore size distribution. The lower thermal energy limits the diffusion of atoms, thereby minimizing the coalescence of smaller pores into larger ones. As a result, the pore size distribution remains more uniform and closer to the original unimodal distribution in the smaller mesopore range.

In this study, the calcination parameters, such as temperature and holding time, significantly influence the textural properties of calcia powders, including BET surface area, pore volume, and pore size as previously described. These findings align with the general trend reported by Chuakam et al. [31], who observed that bio-calcia products derived from calcination at 800 °C for 4 hours exhibited BET surface areas in the range of 3.77–4.96 m^2/g, pore volumes between 0.010–0.027 cm^3/g, and pore sizes ranging from 11.20–22.20 nm. Compared to Chuaka et al. [31], our study demonstrates that higher calcination temperatures (900–1000 °C) and prolonged holding times further reduce the BET surface area and pore volume while increasing average pore radius, indicating the impact of sintering and grain growth during prolonged calcination. These differences underscore the critical role of calcination parameters in tailoring the textural properties of calcia, which can be optimized based on the desired application.

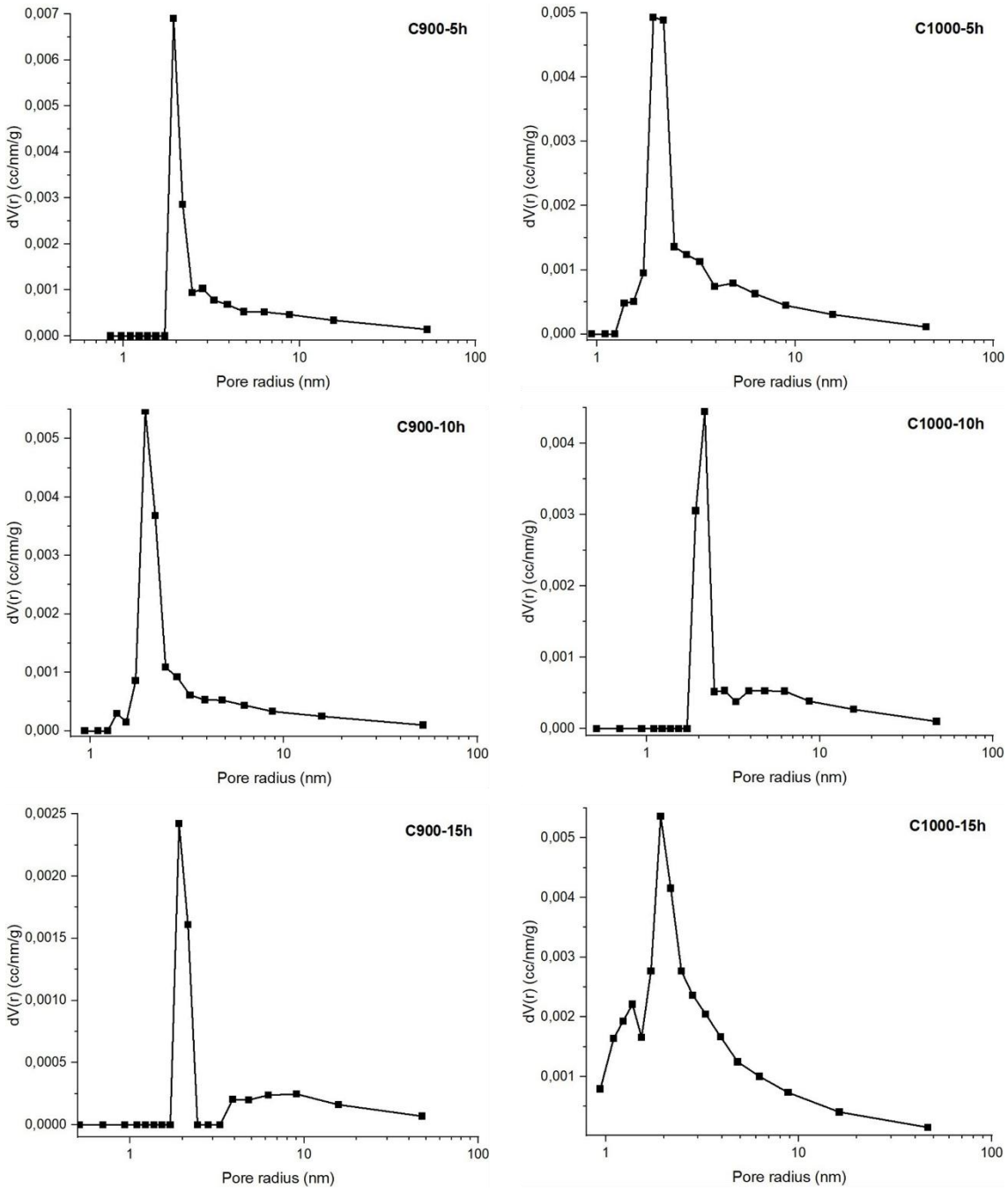

Figure 6. Pore radius distribution of the calcined calcia powders with variation of calcination temperature and holding time

Microstructure Analysis

The SEM analysis of calcia powder calcined at various temperatures and holding times reveals insights into how these factors influence its microstructure, see Figure 7 and 8. At 900 °C, the microstructure of the calcia powder appearing irregular and less defined. In terms of particle size, lower temperatures like 900 °C result in smaller and more dispersed particles, whereas at 1000 °C, the particles grow larger as the higher temperature facilitates coalescence and growth.

Agglomeration also follows a similar trend; at 900 °C, the particles have insufficient energy to bond strongly, leading to less agglomeration. Conversely, at 1000 °C, the enhanced particle mobility causes significant agglomeration as particles cluster together. Calcination holding time further influences these characteristics. With shorter holding times, such as 5 hours, the microstructure remains less well-developed, and the particles are smaller and less uniform due to insufficient growth time. As the holding time increases, the microstructure becomes more defined, with larger and more uniform particles. Agglomeration also increases with longer holding times, as particles have more time to interact and bond, leading to stronger inter-particle bonding.

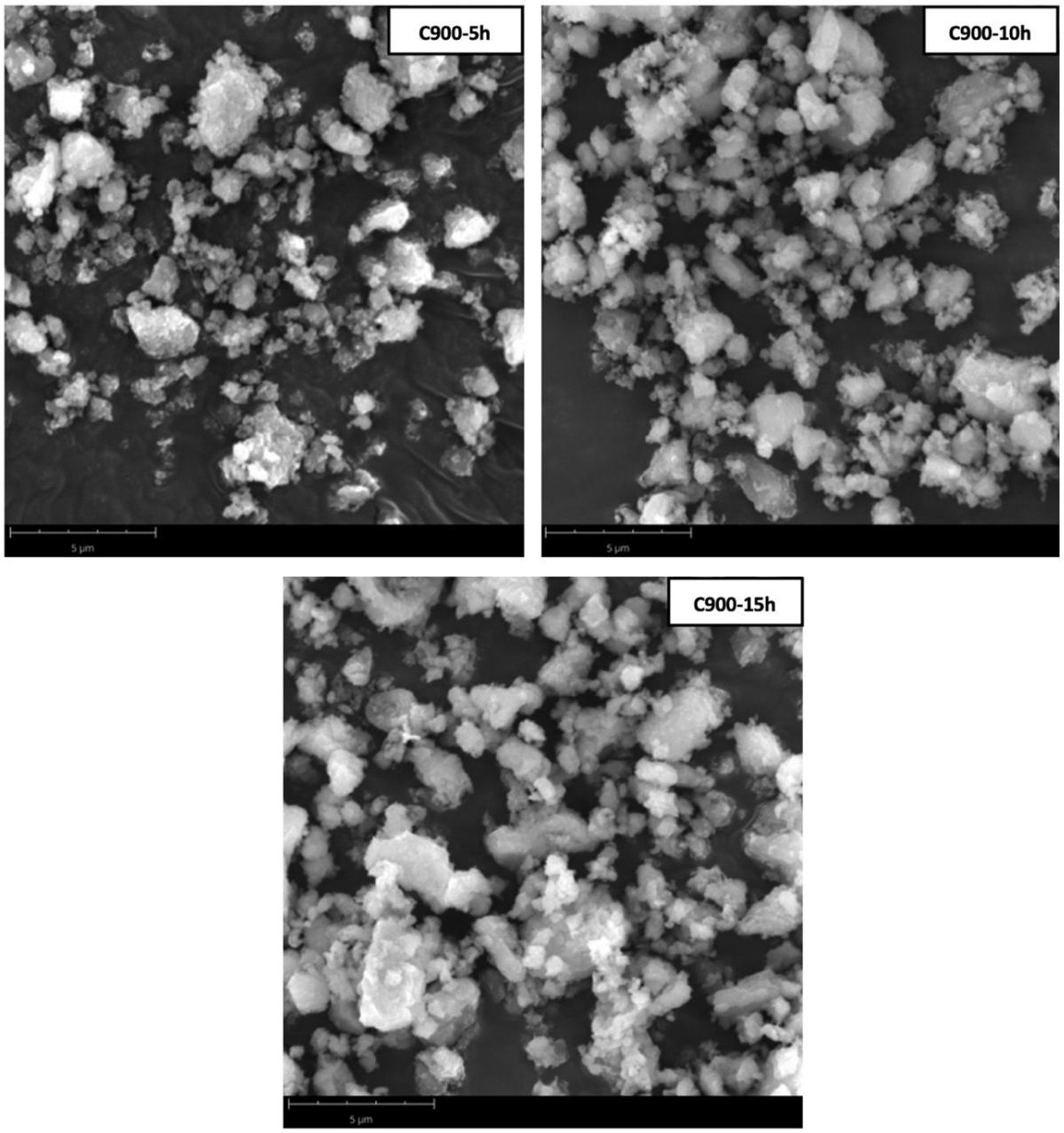

Figure 7. SEM figures of calcia powders calcined at 900 °C with variation of holding time for 5, 10, and 15 hours

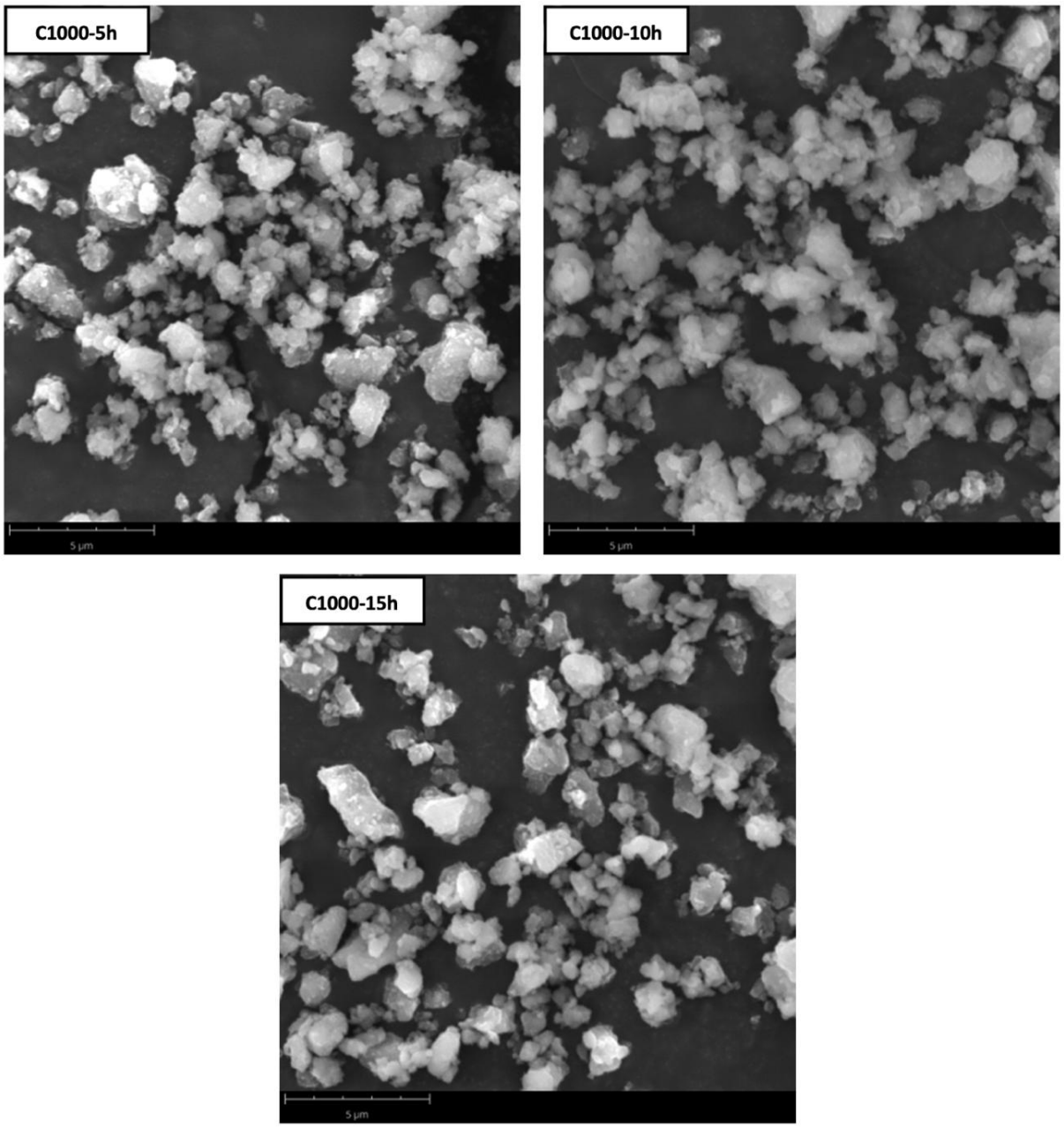

Figure 8. SEM figures of calcia powders calcined at 1000 °C with variation of holding time for 5, 10, and 15 hours

Conclusion

This manuscript explores the influence of calcination temperature and holding time on calcia powders synthesized from chicken eggshell waste. Calcia powders were calcined at 900°C and 1000°C for 5, 10, and 15 hours. Results show that higher temperatures and extended holding times significantly impact calcia powders' structural properties, enhancing sintering and grain growth, reducing average pore radius and total pore volume, and decreasing BET surface area. BJH analysis indicates that longer holding times broaden pore size distribution due to the merging of smaller pores. SEM revealed more defined particles with significant agglomeration at higher temperatures and longer holding times. This study underscores the importance of optimizing calcination conditions to tailor calcia powders' structural properties for applications, achieving desired balances between particle size, surface area, and pore size distribution for enhanced functional performance in industrial contexts. Future research is needed to optimize other calcination parameters, such as heating rate and alternative calcination techniques to further optimize the structural properties of calcium powder.

Acknowledgment

This research was financially supported by the Ministry of Research Technology and Higher Education of the Republic of Indonesia and the Institute for Research and Community Services Uniba under the PDP program Number KTR-05/LPPM-UNIBA/VI/2024 awarded to the principal author.

References

[1] N. A. Zul, S. Ganesan, T. S. Hamidon, W.-D. Oh, and M. H. Hussin, "A review on the utilization of calcium oxide as a base catalyst in biodiesel production," *J. Environ. Chem. Eng.*, vol. 9, no. 4, p. 105741, Aug. 2021, doi: 10.1016/j.jece.2021.105741.

[2] T. Pagar, S. Ghotekar, S. Pansambal, R. Oza, and B. P. Marasini, "Facile Plant Extract Mediated Eco-Benevolent Synthesis and Recent Applications of CaO-NPs: A State-of-the-art Review," *J. Chem. Rev.*, vol. 2, no. 3, pp. 201–210, Jun. 2020, doi: 10.22034/jcr.2020.107355.

[3] X. Zhang *et al.*, "A review on granulation of CaO-based sorbent for carbon dioxide capture," *Chem. Eng. J.*, vol. 446, p. 136880, Oct. 2022, doi: 10.1016/j.cej.2022.136880.

[4] V. K. Yadav *et al.*, "The Processing of Calcium Rich Agricultural and Industrial Waste for Recovery of Calcium Carbonate and Calcium Oxide and Their Application for Environmental Cleanup: A Review," *Appl. Sci.*, vol. 11, no. 9, Art. no. 9, Jan. 2021, doi: 10.3390/app11094212.

[5] R. Nurlaila, Musyarofah, N. F. Muwwaqor, Triwikantoro, A. Kuswoyo, and S. Pratapa, "Phase analysis of ZrO2-SiO2 systems synthesized through Ball milling mechanical activations," *AIP Conf. Proc.*, vol. 1788, no. 1, p. 030122, Jan. 2017, doi: 10.1063/1.4968375.

[6] G. Elsandika, A. D. C. Putri, M. Musyarofah, and S. Pratapa, "Synthesis of $ZrSiO_4$ powders by a sol-gel method with varied calcination temperatures," *IOP Conf. Ser. Mater. Sci. Eng.*, vol. 496, p. 012047, May 2019, doi: 10.1088/1757-899X/496/1/012047.

[7] A. Putkham, S. Ladhan, and A. I. Putkham, "Changing of Particle Size and Pore Structures of Calcium Oxide during Calcinations of Industrial Eggshell Waste," *Mater. Sci. Forum*, vol. 998, pp. 90–95, 2020, doi: 10.4028/www.scientific.net/MSF.998.90.

[8] A. H. Prayitno, B. Prasetyo, and A. Sutirtoadi, "Synthesis and characteristics of nano calcium oxide from duck eggshells by precipitation method," *IOP Conf. Ser. Earth Environ. Sci.*, vol. 411, no. 1, p. 012033, Jan. 2020, doi: 10.1088/1755-1315/411/1/012033.

[9] Y. M. Alobaidi, M. M. Ali, and A. M. Mohammed, "Synthesis of Calcium Oxide Nanoparticles from Waste Eggshell by Thermal Decomposition and their Applications," *Jordan J. Biol. Sci.*, vol. 15, no. 2, pp. 269–274, 2022, doi: 10.54319/jjbs/150215.

[10] J. S. J. Ling, Y. H. Tan, N. M. Mubarak, J. Kansedo, A. Saptoro, and C. Nolasco-Hipolito, "A review of heterogeneous calcium oxide based catalyst from waste for biodiesel synthesis," *SN Appl. Sci.*, vol. 1, no. 8, p. 810, Jul. 2019, doi: 10.1007/s42452-019-0843-3.

[11] M. Musyarofah *et al.*, "Ultra-dense (Bi, V, B)-oxide-added zircon ceramics fabricated by liquid-phase assisted spark plasma sintering (SPS)," *Mater. Res. Express*, vol. 10, no. 5, p. 055002, May 2023, doi: 10.1088/2053-1591/acd521.

[12] N. Nurhayati, M. Musyarofah, S. Rahastama, D. M. Shoodiqin, B. Prayitno, and N. Puspitasari, "Study of The Effect of Calcination Temperature on the Phase Composition of ZnO Powder Synthesized via The Sol-Gel Method," *J. ILMU Fis. Univ. ANDALAS*, vol. 16, no. 1, Art. no. 1, Feb. 2024, doi: 10.25077/jif.16.1.71-78.2024.

[13] B. Peceño, B. Alonso-Fariñas, L. F. Vilches, and C. Leiva, "Study of seashell waste recycling in fireproofing material: Technical, environmental, and economic assessment," *Sci. Total Environ.*, vol. 790, p. 148102, Oct. 2021, doi: 10.1016/j.scitotenv.2021.148102.

[14] N. Azmi, S. Yusup, and K. M. Sabil, "Effect of water onto porous CaO for CO2 adsorption: Experimental and extended isotherm model," *J. Clean. Prod.*, vol. 168, pp. 973–982, Dec. 2017, doi: 10.1016/j.jclepro.2017.08.225.

[15] Q. Song, X. Zha, M. Gao, and Y. Ma, "Influence of raw material purity on microstructure and properties of calcia refractory," *J. Eur. Ceram. Soc.*, vol. 44, no. 3, pp. 1847–1855, Mar. 2024, doi: 10.1016/j.jeurceramsoc.2023.10.051.

[16] P. Kashyap, M. Brzezińska, N. Keller, and A. M. Ruppert, "Influence of Impurities in the Chemical Processing Chain of Biomass on the Catalytic Valorisation of Cellulose towards γ-Valerolactone," *Catalysts*, vol. 14, no. 2, Art. no. 2, Feb. 2024, doi: 10.3390/catal14020141.

[17] N. Uporova and L. Leonova, "Investigation of the impurity effect on the kinetics of thermal decomposition of natural gypsum at high temperatures," *Results Chem.*, vol. 12, p. 101867, Dec. 2024, doi: 10.1016/j.rechem.2024.101867.

[18] D. Wang, C. Shi, N. Farzadnia, Z. Shi, H. Jia, and Z. Ou, "A review on use of limestone powder in cement-based materials: Mechanism, hydration and microstructures," *Constr. Build. Mater.*, vol. 181, pp. 659–672, Aug. 2018, doi: 10.1016/j.conbuildmat.2018.06.075.

[19] Musyarofah, E. F. Damanik, A. R. Septiana, D. M. Shoodiqin, Husain, and G. Yudoyono, "Phase study of Mg1-xZnxTiO3 powders prepared by dissolved metals mixing method," *AIP Conf. Proc.*, vol. 2652, no. 1, p. 050013, Nov. 2022, doi: 10.1063/5.0106315.

[20] K. R. Hallam, J. E. Darnbrough, C. Paraskevoulakos, P. J. Heard, T. J. Marrow, and P. E. J. Flewitt, "Measurements by x-ray diffraction of the temperature dependence of lattice parameter and crystallite size for isostatically-pressed graphite," *Carbon Trends*, vol. 4, p. 100071, Jul. 2021, doi: 10.1016/j.cartre.2021.100071.

[21] L. Huang, G. Cheng, and S. Huang, "Effects of Calcination Conditions on the Formation and Hydration Performance of High-Alite White Portland Cement Clinker," *Materials*, vol. 13, no. 3, Art. no. 3, Jan. 2020, doi: 10.3390/ma13030494.

[22] J. M. Valverde, P. E. Sanchez-Jimenez, and L. A. Perez-Maqueda, "Limestone Calcination Nearby Equilibrium: Kinetics, CaO Crystal Structure, Sintering and Reactivity," *J. Phys. Chem. C*, vol. 119, no. 4, pp. 1623–1641, Jan. 2015, doi: 10.1021/jp508745u.

[23] M. A. Al-Ghouti and D. A. Da'ana, "Guidelines for the use and interpretation of adsorption isotherm models: A review," *J. Hazard. Mater.*, vol. 393, p. 122383, Jul. 2020, doi: 10.1016/j.jhazmat.2020.122383.

[24] H. Mangal, A. Saxena, A. S. Rawat, V. Kumar, P. K. Rai, and M. Datta, "Adsorption of nitrobenzene on zero valent iron loaded metal oxide nanoparticles under static conditions," *Microporous Mesoporous Mater.*, vol. 168, pp. 247–256, Mar. 2013, doi: 10.1016/j.micromeso.2012.10.006.

[25] D. P. Lapham and J. L. Lapham, "Gas adsorption on commercial magnesium stearate: Effects of degassing conditions on nitrogen BET surface area and isotherm characteristics," *Int. J. Pharm.*, vol. 530, no. 1, pp. 364–376, Sep. 2017, doi: 10.1016/j.ijpharm.2017.08.003.

[26] Y. Zhao *et al.*, "Effects of calcination temperature on grain growth and phase transformation of nano-zirconia with different crystal forms prepared by hydrothermal method," *J. Mater. Res. Technol.*, vol. 19, pp. 4003–4017, Jul. 2022, doi: 10.1016/j.jmrt.2022.06.137.

[27] S.-B. Lee, E.-H. Ko, J. Y. Park, and J.-M. Oh, "Mixed Metal Oxide by Calcination of Layered Double Hydroxide: Parameters Affecting Specific Surface Area," *Nanomaterials*, vol. 11, no. 5, Art. no. 5, May 2021, doi: 10.3390/nano11051153.

[28] Z. Ž. Vasiljević *et al.*, "Exploring the impact of calcination parameters on the crystal structure, morphology, and optical properties of electrospun Fe 2 TiO 5 nanofibers," *RSC Adv.*, vol. 11, no. 51, pp. 32358–32368, 2021, doi: 10.1039/D1RA05748K.

[29] J. P. Ramos, C. M. Fernandes, T. Stora, and A. M. R. Senos, "Sintering kinetics of nanometric calcium oxide in vacuum atmosphere," *Ceram. Int.*, vol. 41, no. 6, pp. 8093–8099, Jul. 2015, doi: 10.1016/j.ceramint.2015.03.007.

[30] R. Han *et al.*, "Progress in reducing calcination reaction temperature of Calcium-Looping CO2 capture technology: A critical review," *Chem. Eng. J.*, vol. 450, p. 137952, Dec. 2022, doi: 10.1016/j.cej.2022.137952.

[31] S. Chuakham *et al.*, "Scalable production of bio-calcium oxide via thermal decomposition of solid - hatchery waste in a laboratory-scale rotary kiln," *Sci. Rep.*, vol. 15, no. 1, p. 865, Jan. 2025, doi: 10.1038/s41598-024-84889-w.